Effect of processing routes and defects on magnetic properties of τ $L1_0$ MnAl alloys

Sujit Desai and Amanda Krause, PhD
Material Science and Engineering
University of Florida, Gainesville, FL, USA

***Abstract* - In this paper effect of different processing routes and resultant microstructural defects on the magnetic properties of τ MnAl alloys was studied. MnAl was found to be the best manganese compound to make permanent magnets. Deformation processing favored the coercivity but severely affected the saturation magnetization. The microstructure of the τ phase had Twin defects. These defects promoted the reverse phase domain nucleation and hampered the realization of large coercivity. The impurities in the alloys formed precipitates which brought about a pinning effect that enhanced the coercivity. Overall, a twin-free material with high dislocation density or a large number of nano precipitates was deemed to be crucial for better permanent magnets.**

Introduction

Magnets constitute an indispensable part of the industrialized world. Their application in motors, generators, tape recorders, magnetic reading, and writing was made possible due to the continuous development of new alloys and materials with improved properties. Maximum energy product, the maximum product of applied field (H) and induced magnetization(M) in a magnet, doubled almost every 12 years and core losses halved every 15 years reaching negligible value. Also, the density of the magnetic record on the hard disk saw 'Moore's Law' type growth. [1]

The timeline of magnetic material development shows that magnets began to improve with the development of 'Hard' magnetic materials like Alnico. [2] Hard magnets have high coercivity (H_C). Coercivity is the amount of magnetic field need to be applied on a magnetized material to remove its magnetization. The Alnico development was followed by a breakthrough discovery of hexagonal ferrites in the 1950s and Rare earth alloys like $SmCo_5$ in the 1960s. But, the erratic supply of rare earth made scientists focus on the development of magnetic compounds with transition metals. This effort led to the development of Manganese alloys and

a

Structure	MnAl $L1_0$	MnBi $B8_1$	Mn_2Ga $D0_{22}$	Mn_3Ga $D0_{22}$	Mn_3Ge $D0_{22}$
T_C (K)	650	633	>770	>770	>865
M_S (M Am^{-1})	0.6	0.58	0.47	0.18	0.07
K_1 (M Jm^{-3})	1.7	0.9	2.35	1.0	0.91
Cost ($/Kg)	4	15	120	90	540

b

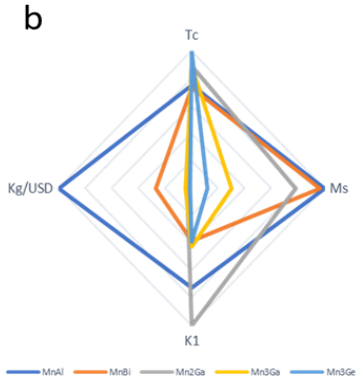

Figure 1: a. Properties of different manganese compounds. b. Normalized property polygon of Manganese Compounds.

the optimization of their microstructure for better coercivity and better maximum energy product. [1] However, this work was interrupted by the development of $Nd_2Fe_{14}B$. The Nd-Fe-B alloys had high magnetocrystalline anisotropy and saturation magnetization due to Nd, high curie temperature due to Fe, and uniquely stable tetragonal structure due to minor addition of Boron. Saturation magnetization is the maximum attainable magnetization in a magnet when placed in a uniform magnetic field. Some materials have different saturation magnetization in different crystallographic directions. This is known as magnetocrystalline anisotropy. Curie temperature is the threshold temperature after which a ferromagnetic material shows paramagnetic behavior. The optimization of maximum energy products has been stagnant since the discovery of Nd-Fe-B alloy and the alloy itself has little scope to improve that parameter.

Also, the gap between the maximum energy product of Nd-Fe-B (400 KJ m^{-3}) and best ferrite magnets (<40 KJ m^{-3}) is unfilled. This gap suggests opportunities to develop the Mn-based magnets which went out of focus due to Nd-Fe-B alloy development. Thus, efforts are poured into developing Mn-based magnets with cheaper alloying elements from group III, IV, and V and interstitial addition of N, C, and B. [3, 4]

Manganese had always been an option to make a better magnet due to its ability to carry a large magnetic moment. Mn can bear a 3.7 Bohr-magnetron magnetic moment. [1] However, the real problem is to carefully control the Mn-Mn atomic separation. Manganese forms a unit cell with

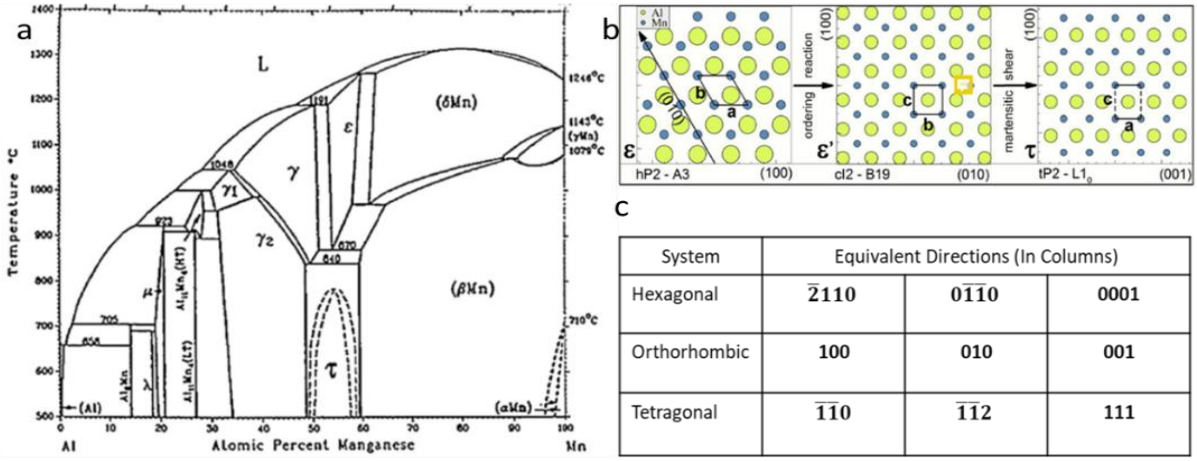

System	Equivalent Directions (In Columns)		
Hexagonal	$\bar{2}110$	$01\bar{1}0$	0001
Orthorhombic	100	010	001
Tetragonal	$\bar{1}10$	$\bar{1}12$	111

Figure 2: a. Phase diagram of MnAl system. b. η to τ phase transformation of MnAl alloy. c. Equivalent directions of different phases of MnAl alloys

4 different sites containing Mn atoms carrying a magnetic moment. Direct magnetic exchange coupling in a half-filled d-band in manganese is naturally Antiferromagnetic. Also, the hybridization with the nearest neighbor atom reduces the magnetic moment. Among those 4 sites, only atoms on the sites with bond distance > 290 nm have a larger magnetic moment that can couple ferromagnetically. But the large separation between those atoms reduces the Magnetization which is a magnetic moment per unit volume.

To address this issue and problems associated with some promising Mn compounds, Coey et. al. reviewed studies of MnAl, MnBi, MnGa, MnGe alloys. Out of them, MnAl proved to have the most favorable balance of magnetic properties as shown in figure 1.

In the light of all the research invested to study MnAl alloys, this paper reviews literature namely about the synthesis of Magnetic MnAl alloy, the crystal structure and microstructure evolution of its magnetic τ phase, defects in the microstructure, and its effect on the magnetic properties of the alloy.

Phase Transformation

The τ phase of the MnAl alloy system is magnetically active. It is meta-stable and is derived from the high temperature η phase. Figure 2.a represents the phase diagram of the alloy system.

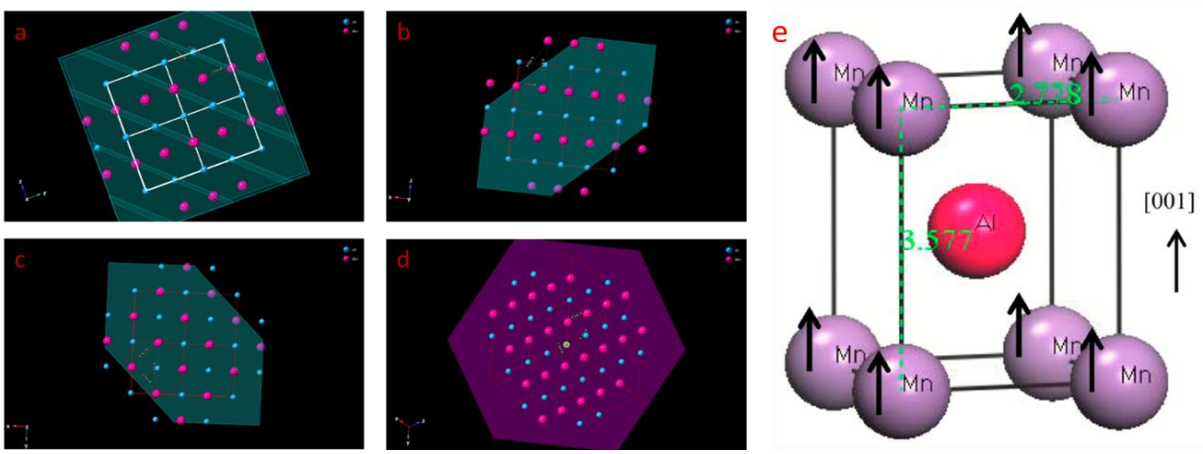

Figure 3: Crystal structure of τ MnAl phase viewed from a. (100) b. (010) c. (001) and d. (111) directions. e. tP2 structure of τ MnAl phase with lattice parameters

[5] The τ phase is bounded by the β and γ_2 phases suggesting that only the alloys with Mn composition between 50 - 60 at. % can realize the τ phase. Kono et. al. suggested that there is a change in the solubility of the β and γ_2 phases below temperatures 840 ° C, which might have created a miscibility gap between these two phases (between Mn composition of 50 – 60 at. %) giving rise to a metastable τ phase. [6]

Jacubovics et. al. suggested that τ phase can be obtained by quenching the samples with high temperature η phase (HCP structure), to room temperature and performing annealing at temperatures between 400° C and 600° C.

He explained that the high temperature η phase is a disordered close-packed hexagonal structure which, when quenched to room temperature, is converted to an intermediate orthorhombic η' phase which has some degree of order. [7] This very η' phase gets converted into the final ferromagnetic τ phase upon annealing. The equivalent directions and planes from these three phases can be inferred from figure 2.c. The stepwise transformation is given in figure 2.b. [8]

The resultant τ phase crystal structure can further be imagined either as BCC equivalent (Pearson symbol: tP2) or FCC equivalent (Pearson symbol: tP4) tetragonal structure. [9] The

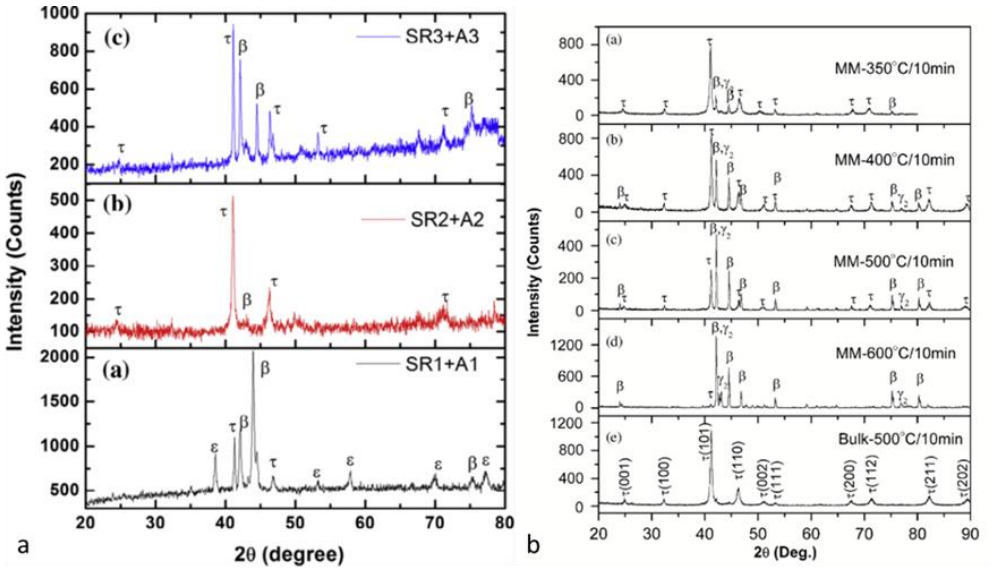

Figure 4: a. Diffraction patterns of MnAl alloys processed by SR1+A1, SR2 + A2, and SR3 + A3 routes. b. Diffraction patterns of MnAl alloys processed by Bulk and MM routes.

tP2 has 2 atoms per unit cell and tP4 has 4 atoms per unit cell. The schematics of the tP4 structure represented in figure 3.a-3.d has been constructed in the crystal maker.

Wei et.al., calculated the site occupancy of Mn and Al in a tP2 unit cell using $Mn_{54}Al_{46}$, $Mn_{51}Al_{46}C_3$ samples. Authors suggested that the majority of 1*a* (0, 0, 0) positions are occupied by Mn, and 1*d* (½, ½, ½) sites are occupied by Al and C. From figure 3.e (attach figure 1 from Wei's 2014 paper), it is clear that the distance between 1*a* positions along the magnetically easy *c*-axis is greater than 290 pm. Thus, this configuration can be expected to produce ferromagnetic Mn-Mn coupling. [10]

Processing Routes

As mentioned in the earlier section, the realization of the τ phase is practically possible only by annealing the as-quenched samples. Jacubovics et. al. carefully examined the microstructure of as-quenched samples and those of samples annealed at 450 °C for 15 mins, 1 h, and 4 h respectively. The as-quenched samples had no features in a diffraction pattern that were suggestive of the τ phase. [11] After 15 mins of annealing, peaks were still predominantly η'. After 1 h of annealing, the microstructure showed a dense distribution of small τ phase nuclei.

These changes were also witnessed in the diffraction pattern. For 4 h annealed samples, the diffraction pattern showed the presence of τ phase with a larger grain size. The authors also recorded the corresponding change in saturation magnetization. It can be believed, from these results, that saturation magnetization is directly impacted by the fraction of the τ phase present in samples.

Singh et. al. studied the effect of mechanical deformation on the magnetic properties of the samples. Authors prepared samples from ball milling (SR1 + A1), arc melting (SR2 + A2), and a combination of arc melting and ball milling (SR3 + A3). All of the samples were annealed further to realize the τ phase. Authors found that only in the case of arc melting the annealed sample had τ phase as the only dominant component. We can see from figure 4.a that the ball milling route had the β phase as a majority component whereas the melting + milling route had comparable amounts of τ and β phases. Room temperature hysteresis loop studies reflect very low saturation magnetization in the case of ball-milled samples. This further confirmed that, since the τ phase is the only ferromagnetic phase in the MnAl system, a high amount of τ phase is crucial for higher values of saturation magnetization. The η' phase has three orientational variants and only one of them to can be transformed into the τ phase. [12] Ball milling activates multiple slip systems in the room temperature mixture of η + η'. And if this mixture has one or more variants of η' then the transformation to τ phase will not be efficient. Further, according to authors, defects introduced by ball milling favored η + η' to β transformation over η + η' to τ transformation.

Zeng et. al. gauged the effect of annealing temperatures on the τ phase. Authors performed mechanical milling on the quenched-annealed samples and recorded the diffraction peaks by employing different annealing temperatures on the mechanically milled (MM) samples. [13] Figure 4.b shows the diffraction peaks. As the annealing temperature was increased the intensity of τ phase peaks declined sharply and were almost zero at 600 ° C. Authors cited that

a higher number of defects in MM samples creates higher atomic mobility. This higher mobility increases further at higher annealing temperatures and favors the formation of β and γ_2 phases over τ phases.

Bittner et. al. studied the effect of hot-extrusion on the texture of MnAl and its magnetic properties. [9] Figure 5 shows the inverse-pole figure of hot-extruded samples. Most of the crystals in the sample can be seen to align along [001] direction (extrusion direction and also the magnetically easy axis of MnAl) confirming the presence of texture. As a result, the Remanence and coercivity are higher when measured along the extrusion direction. The calculated texture value for the hot extruded sample was ω = 0.45, which suggested medium texture.

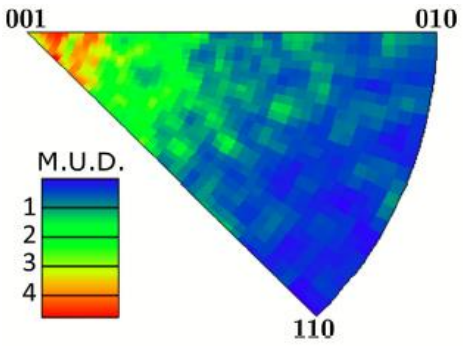

Figure 5 : EBSD-derived inverse pole figure for the hot extruded sample showing the distribution of crystallographic poles parallel to the extrusion direction.

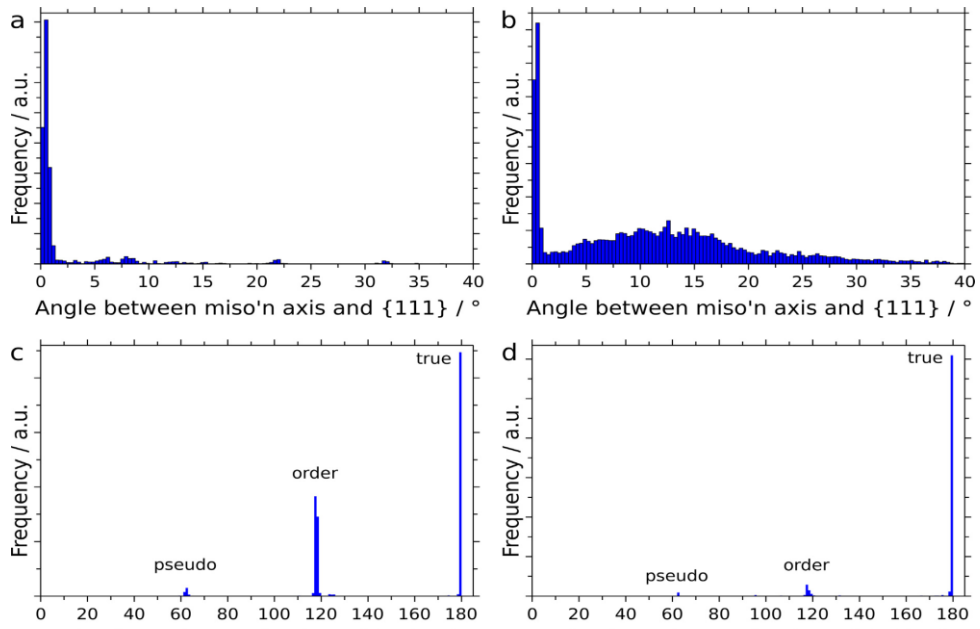

Figure 6: Angle between the misorientation axis (miso'n axis) and the nearest {111} pole in (a) the as-transformed sample and (b) the hot extruded sample for all misorientations where the disorientation angle was >5°. Distribution of misorientation angles for all misorientations where the disorientation angle was >5° and the angle between the misorientation axis and the nearest {111} pole was <2° for (c) the as-transformed sample and (d) the hot extruded sample.

Microstructure and Defects

Twins and APBs:

The actual decisive factor for magnetic properties is not the processing route but the microstructural features it cultivates. Jacubovics et. al. studied the τ phase microstructure of MnAl and confirmed the presence of Stacking Faults (SFs) along ⅙<112> directions on {111} planes. A stacking fault is a disruption in order of a grain/crystal due missing/excess plane of atom. The samples also contained antiphase boundaries (APBs). [7] The areas on the either side of APBs have opposite order of atoms. The SFs had, in some cases, domain walls attached with them and acted as wall pinning sites rather than domain nucleation sites. Pinning sites hinder the movement of grains by pinning its boundaries. These SFs were the areas that might have remnant orthorhombic η' phase. Thus, the presence of such SFs might weaken exchange interaction across them and might be desirable around reverse-phase domain walls. In a magnetic domain of a magnetic material all the grains have same direction of magnetization. Reverse phase domain walls separate two antiparallelly aligned magnetic domains. APBs always had domain walls attached to them. The APBs were believed to act as nucleation sites of reverse domains, which are highly undesirable for a good permanent magnet.

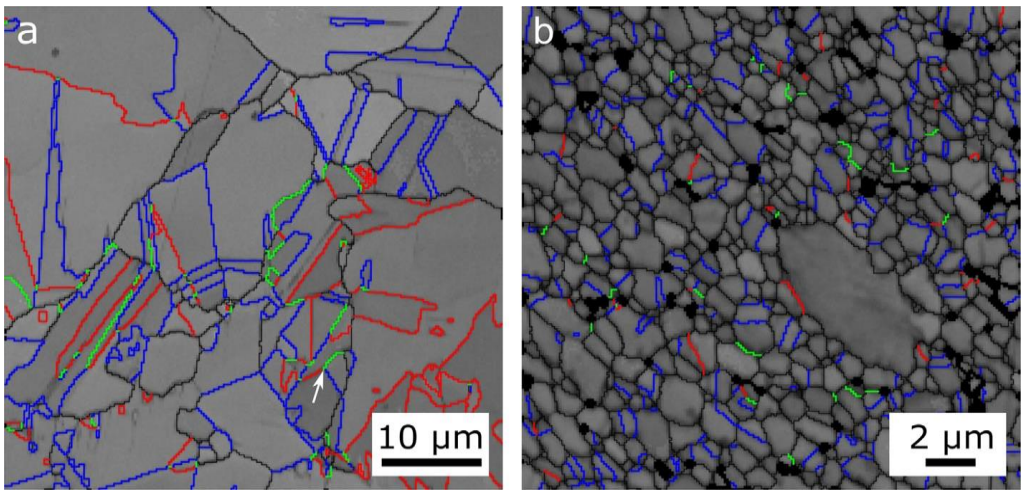

Figure 7: Spatial distribution of the different {111} related interfaces in the different treated samples: (a) as-transformed and (b) hot extruded (The different coloured interfaces correspond to pseudo twins (green), order twins (red) and true twins (blue); other grain boundaries appear black).

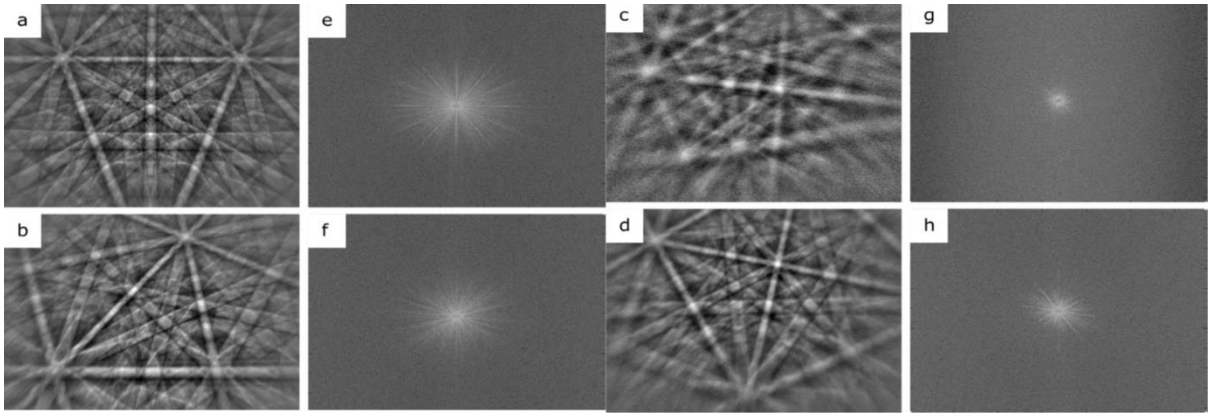

Figure 8: Most representative Kickuchi patterns and 2D-FFT of several metallurgical conditions: (a),(e) transformed by route 1, (b),(f) transformed by route 2, (c),(g) cold-worked by swaging and (d),(h) recovered.

Houseman et. al. studied the effect of carbon impurity addition on microstructure evolution. Authors found that the addition of carbon does not enhance the M_S and M_R values (from that of undoped MnAl). However, the time required to attain these values was considerably large in the case of the Mn-Al-C system.

This confirmed the previously held belief that carbon retards the η to τ transformation. [14] Further, after carbon addition, the APBs were less frequent and sometimes separate from domain walls. [11] This study also confirmed the presence of twins. Twins formed after shearing every {111} plane by ⅙<112> vector. The *c*-axis and 180° domain walls of the twin variants changed their direction across twin boundaries. [11, 15] Domain walls were also present along the twin boundaries.

As technology evolved, these defects were analyzed using advanced microstructure analysis instruments.

Bittner et. al. studied the twins in as-annealed and hot extruded samples and attempted to quantify the misorientation between magnetically easy axes of twin variants across twin boundaries. [9] For both the samples, the majority of the records had their misorientation axis closely aligned with one of {111} equivalent directions. Results are shown in Figures 6.a and 6.b. This confirms the misorientation axis to be {111} in τ MnAl like the one in γ TiAl. [15, 16]

The authors also recorded the misorientation angle distribution of axes aligned with <111> direction. As shown in figure 6.c and 6.d, the highest peaks were recorded at 62°, 118°, and 180° angles corresponding to pseudo twins, ordered twins, and true twins respectively. [9]

The angle between magnetically easy axes of twin-variants on either side of twin boundaries was 48°, 86°, and 75° for pseudo twins, ordered twins, and true twins.

For the as-transformed samples, true twin ordered twin, and pseudo twin fractions were 54 % 41 % and 3%. For the hot extruded sample, it was 84% 7% and 1%. The greater fraction of ordered twins in the as-transformed samples was justified as a result of transformation-strains which induce during η to τ transformation. [16]

Figure 7 shows the presence of triple points in both the samples. The simple rule of misorientation used for FCC lattice was extrapolated for the τ MnAl crystal system. [17] Using this rule, misorientation angles of pseudo twins and ordered twins added exactly to the misorientation angle of true twins. This result was used to assume that pseudo twins may occur due to the interaction of true twins and ordered twins. [9]

Dislocations:

After studying the effect of twins and APBs, the same group of authors investigated the impact of dislocations on coercivity of the τ phase in MnAl. Bittner et. al., employed continuous cooling (route 1), quenching (route 2), cold working (followed by route 1), and cold working-recovering (followed by route 1). Authors found that all the processing routes resulted in samples with twin defects. [18]

Kikuchi diffraction bands and corresponding 2-D Fast Fourier Transforms of all the samples were studied and are shown in figure 8.a-8.d. The thickness of the diffraction band depends on lattice spacing and samples with dislocations and high lattice distortions were expected to have blurred Kikuchi bands. [19] The same was reflected in actual results as shown in figure 8.e-8.h.

For distorted lattice, the radial intensity of the bright central spot decreases sharply with radial distance from the center. The radius of the bright spot was the smallest for the cold-worked sample indicating the highest dislocation density in the cold-worked sample. These dislocations, according to the authors, acted as pinning sites and help in increasing the coercivity of τ MnAl magnets. Thus, authors recommended cold-working or hot-working or a combination of both to realize microstructural features that can enhance the coercivity.

Since the presence of dislocations was deemed crucial, more efforts were invested to realize pinning centers in τ MnAl microstructures to enhance coercivity. Zhao et. al., attempted Tb impurity addition in MnAl samples to create nano-precipitates.

Coercivity vs Tb content graph from the authors' work is shown in figure 9. The coercivity peaks at Tb = 0.2 at. % for the annealed ribbon. There is an overall increase in the coercivity of the samples when processed with mechanical milling. [20] Authors believe that when the defect/precipitate dimension is comparable to the domain wall width, there is a strong pinning effect which might increase the coercivity. Using the anisotropy constant and exchange coupling constant, the calculated value of the domain wall width is 4.2 nm. Precipitates formed in Tb content = 0.2 at. % has the closest value to this. This can be the reason for Tb content = 0.2 at. % to have the highest coercivity. For higher Tb content not only the precipitate size was larger but they are continuously distributed along the grain boundaries. This is believed to weaken the pinning effect.

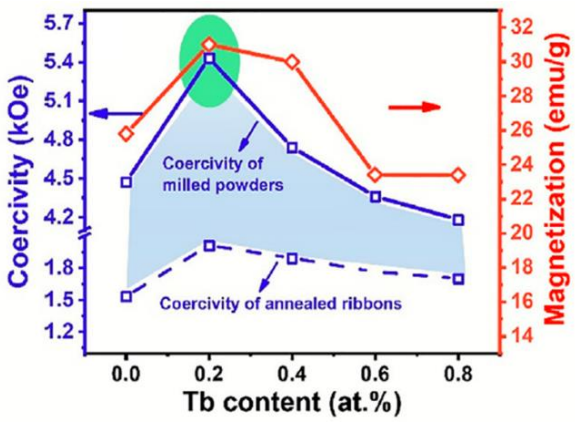

Figure 9: The variation of Hc versus Tb content is exhibited by the blue solid line for as-milled powders and the blue dash line for as-annealed ribbons, the variation of M_{5T} versus Tb content is exhibited by red solid line.

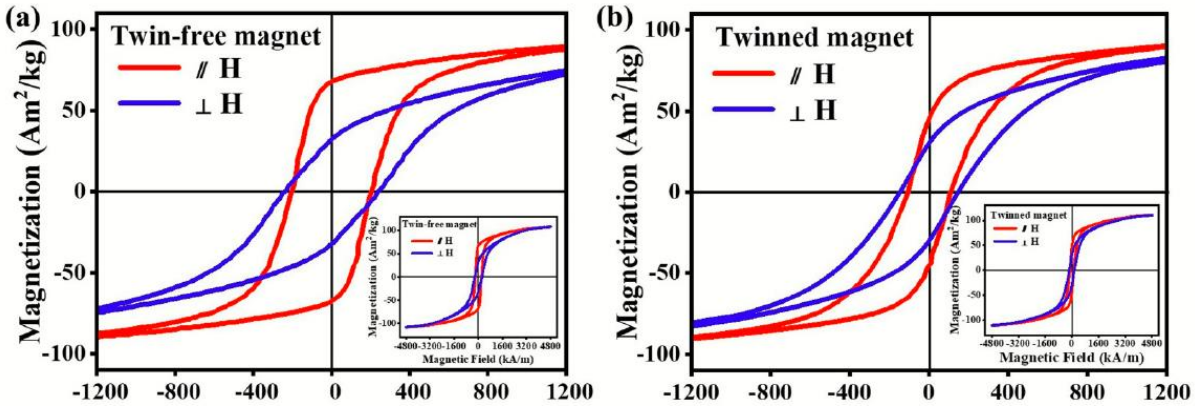

Figure 10: Magnetic hysteresis loops of (a) twin-free magnet and (b) twinned magnet, measured along and perpendicular to the direction of texture at 300 K.

In their latest work, Jia et. al. studied the effects of both the twins and dislocations on the domain walls in τ MnAl magnets to come up with a more complete solution regarding processing route and microstructural features. The authors prepared both the twinned and twin-free samples of almost the same grain size.

Room temperature hysteresis loops of both the twin-free and twinned samples are shown in Figures 10.a and 10.b. The twin free samples had coercivity values twice that of twinned samples in both the cases when the applied external field is parallel and perpendicular to MnAl magnets. Remanence measured in Parallel field also favored the twin free sample. Twin free

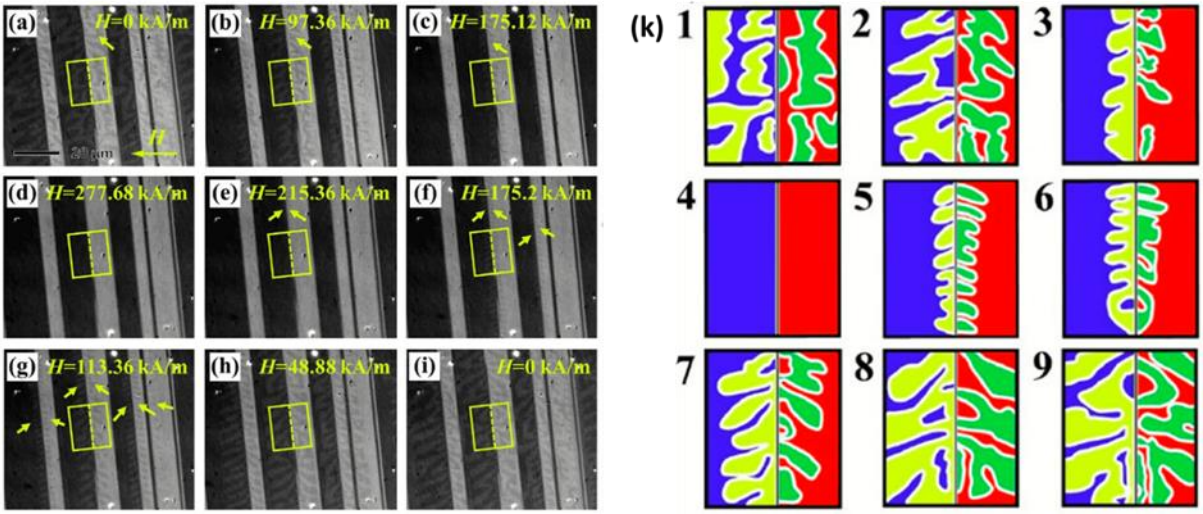

Figure 11: (a–i) MOKE images showing the interaction of domain structures and twin boundaries during magnetization and demagnetization processes in twinnedMnAl alloys. (k) Schematic figures of magnetic domain evolution selected from the yellow rectangle in the MOKE images, corresponding to the data points 1–9 on the curve.

sample values were 60% larger than twinned values. [21] Thus, elimination of twins was confirmed to be beneficial both to coercivity and to remnance.

XRD patterns of twin free samples show strong [001] texture; the high intensity of (001) and (002) along with (101). On the other hand, the twinned sample has the same peak intensity as the standard sample (high intensity of (101)). Analysis of the SAED pattern shows that the twinning plane is (101); The diffraction patterns of two different cells coincide only at (101) planes. The EBSD studies of the twinned sample revealed a large fraction of small-angle boundaries, representing misorientation of 1°-3°, and twin boundaries, with misorientation of 74°-77° between *c*-axis of twin variants. From previous studies of misorientation, we can attribute the presence of true twins to these twin boundaries.

Apart from EBSD and hysteresis loop studies, domain wall motion was analyzed by *in situ* MOKE images. Figure 11.a-11.i represent the actual domain images and figure 11.k represents schematics of actual domain images. The domain walls dissolved and nucleated, in response to an external magnetic field, perpendicular to the twin boundary. Thus, twin sites are confirmed to act as nucleation sites during the demagnetization process and hence reduce the coercivity of the magnets.

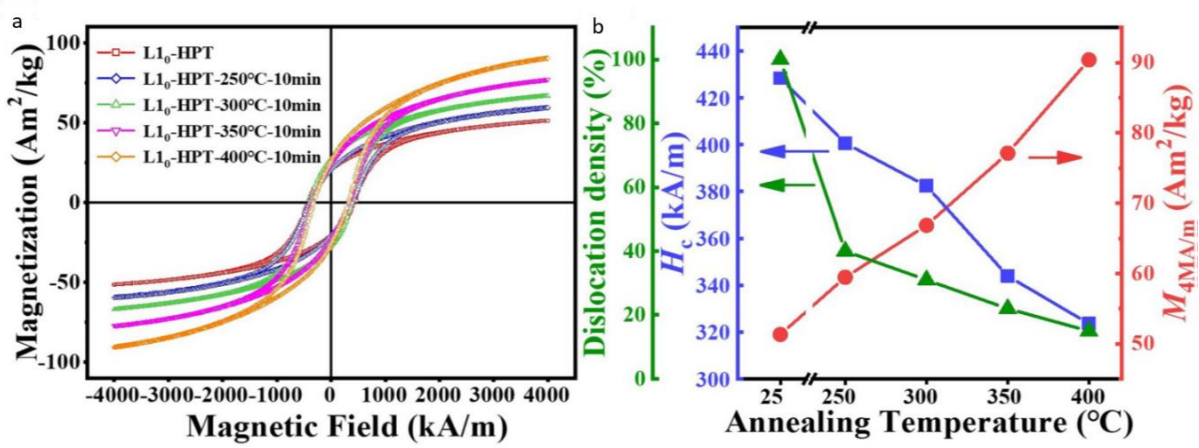

Figure 12: a. Hysteresis loops of L10-MnAl after HPT and series of annealing treatment. b. Evolution of dislocation density, Hc and $M_{4\ MA/m}$ with the different annealing treatment temperature.

Authors compared samples prepared by various routes and found dislocations only in the ball-milled and HPT samples. Since only these two types of samples were believed to have a pinning effect, it was confirmed that pinning centers were necessary to increase the coercivity in the magnets. The pinning field was stronger in the HPT samples than in Ball-milled samples (480 kA/m versus 320 kA/m). Hence HPT samples were used to study the impact of the dislocations on the properties. Also, the HPT samples were annealed at different temperatures to regulate the dislocation density in the samples and gauge its effect on the magnetic properties.

Finally, the room-temperature magnetization curves of samples annealed at different temperatures were measured 12.a. As we can see in the figure 12.b, the magnetization under 4 MA/m field varied from 51 A m^2/kg for after HPT samples to 90 A m^2/kg for 400° C annealing. Lower magnetization in the after-HPT samples can attribute to Mn-Mn Antiferromagnetic coupling resulting from lattice distortion. [22] The results are shown in the figure also confirm the direct correlation between dislocation density and coercivity of the τ MnAl magnets.

Thus, authors concluded that in order to have better magnetic properties, the MnAl magnet microstructure should **1. Be free of twin defects and 2. Have nano precipitates with a high density of dislocations.**

Coercivity Mechanisms

Research studying the coercivity mechanism in magnets suggests that defects affect the nucleation and pinning simultaneously. [22, 23, 24] When defects will reduce the local anisotropic field, the defect site will be conducive for domain wall nucleation and eventual domain reversal. The same defect can also generate magnetic properties gradient and hence might pin the reversal of domains. [21] When the external magnetic field overcomes the pinning field, the domain reversal takes place through domain wall nucleation.

In the presence of twin defects, the anisotropic field is lowered. Since there is little difference in the magnetic parameters of perfect lattice and twins, the pinning effect is negligible and the pinning field is almost unchanged. Hence in the presence of twins, the coercivity is severely hampered due to lowering of anisotropic field and absence of strong pinning effect. [21] In the presence of dislocations, the nucleation field (energy required to nucleate the reverse domains) is decreased but the energy required to depin the walls is increased at the same time (pinning field is lowered). Thus, increasing coercivity in the deformed magnet.

Conclusion

In this work, the evolution of Magnetic materials and the path to discovery of rare-earth free magnets, especially MnAl magnets was visited. The crystal structure of τ MnAl phase, the phase transformation process, and processing routes were studied. The case studies using different analysis techniques to investigate τ phase microstructural features were reviewed. All these studies confirmed the presence of twins and dislocations as ubiquitous microstructural features. To manufacture good quality τ MnAl magnets, the presence of twins was deemed as undesirable and the presence of dislocation as necessary. To date, no work has been done in the areas of grain boundary engineering of τ phase. We might witness new research in this direction.

References

1. Coey JMD. New permanent magnets; manganese compounds. J Phys Condens Matter. 2014;26(6):064211.
2. Coey JMD. Magnetism and magnetic materials [Internet]. Cambridge, England: Cambridge University Press; 2012.
3. Coey JMD. Permanent magnets: Plugging the gap. Scr Mater. 2012;67(6):524–9

4. Coey JMD. Hard magnetic materials: A perspective. IEEE Trans Magn. 2011;47(12):4671–81.
5. Cahn RW. Binary Alloy Phase Diagrams-Second edition. T. B. Massalski, Editor-in-Chief; H. Okamoto, P. R. Subramanian, L. Kacprzak, Editors. ASM International, Materials Park, Ohio, USA. December 1990. xxii, 3589 pp., 3 vol., Adv Mater. 1991;3(12):628–9.
6. Kōno H. On the ferromagnetic phase in manganese-aluminum system. J Phys Soc Jpn. 1958;13(12):1444–51.
7. Jakubovics JP, Jolly TW. The effect of crystal defects on the domain structure of Mn-Al alloys. Physica. 1977;86–88:1357–9.
8. Janotová I, Švec P Sr, Švec P, Mat'ko I, Janičkovič D, Zigo J, et al. Phase analysis and structure of rapidly quenched Al-Mn systems. J Alloys Compd. 2017;707:137–41
9. Bittner F, Schultz L, Woodcock TG. Twin-like defects in L10 ordered τ-MnAl-C studied by EBSD. Acta Mater. 2015; 101:48–54.
10. Wei JZ, Song ZG, Yang YB, Liu SQ, Du HL, Han JZ, et al. τ-MnAl with high coercivity and saturation magnetization. AIP Adv. 2014;4(12):127113.
11. Houseman EL, Jakubovics JP. Domain structure and magnetization processes in MnAl and MnAlC alloys. J Magn Magn Mater. 1983;31–34:1005–6.
12. Singh N, Mudgil V, Anand K, Srivastava AK, Kotnala RK, Dhar A. Influence of processing on structure property correlations in τ-MnAl rare-earth free permanent magnet material. J Alloys Compd. 2015; 633:401–7.
13. Zeng Q, Baker I, Cui JB, Yan ZC. Structural and magnetic properties of nanostructured Mn–Al–C magnetic materials. J Magn Magn Mater. 2007; 308(2):214–6
14. The Matsushita Electric Industrial Co. Ltd. UK. Patent.1473002.

15. Houseman EL, Jakubovics JP. Electron microscope study of the domain structure of MnAlC magnets. J Magn Magn Mater. 1983;31–34:1007–8.
16. Feng CR, Michel DJ, Crowe CR. Twin relationships in TiAl. Scr Metall. 1988;22(9):1481–6.
17. Ranganathan S. On the geometry of coincidence-site lattices. Acta Crystallogr. 1966;21(2):197–9.
18. Bittner F, Freudenberger J, Schultz L, Woodcock TG. The impact of dislocations on coercivity in L10-MnAl. J Alloys Compd. 2017;704:528–36.
19. Yamaguchi M, Umakoshi Y. The deformation behavior of intermetallic superlattice compounds, Prog. Mater Sci. 1991;34:1–148.
20. Zhao S, Wu Y, Wang J, Jia Y, Zhang T, Zhang T, et al. Realization of large coercivity in MnAl permanent-magnet alloys by introducing nano precipitates. J Magn Magn Mater. 2019;483:164–8.
21. Jia Y, Wu Y, Zhao S, Zuo S, Skokov KP, Gutfleisch O, et al. L10 rare-earth-free permanent magnets: The effects of twinning versus dislocations in Mn-Al magnets. Phys Rev Mater. 2020;4(9).
22. Zhao GP, Wang XL, Yang C, Xie LH, Zhou G. Self-pinning: Dominant coercivity mechanism in exchange-coupled permanent/composite magnets. J Appl Phys. 2007;101(9):09K102.
23. Zhao GP, Zhao L, Shen LC, Zou J, Qiu L. Coercivity mechanisms in nanostructured permanent magnets. Chin Physics B. 2019;28(7):077505.
24. Zhao GP, Zhang HW, Feng YP, Yang C, Huang CW. Nucleation or pinning: Dominant coercivity mechanism in exchange-coupled permanent/composite magnets. Comput Mater Sci. 2008;44(1):122–6.